PROCEEDINGS, Thirty-Sixth Workshop on Geothermal Reservoir Engineering
Stanford University, Stanford, California, January 31 - February 2, 2011
SGP-TR-191

FRACTURES INTERPRETED FROM ACOUSTIC FORMATION IMAGING TECHNOLOGY: CORRELATION TO PERMEABILITY

K. McLean[1] and D. McNamara[2]

[1]Contact Energy, Wairakei Power Station, Private Bag 2001, Taupo 3352, NZ
katie.mclean@contactenergy.co.nz
[2]GNS Science, Wairakei Research Centre, Private Bag 2000, Taupo 3352, NZ
D.Mcnamara@gns.cri.nz

ABSTRACT

Permeable feed zones in geothermal wells are commonly identified using well profiles of temperature, pressure and fluid velocity measured at different injection rates during well completion testing and heat-up. While this data gives some indication of the depth and relative strength of the feed zones it does not give any information on the nature of the permeability in those zones, be it primary or secondary. Fracturing is thought to contribute to permeability in areas targeted for deep reinjection in the Wairakei geothermal system, within the Tahorakuri and Waikora Formations. By characterizing those deep fractures in terms of orientation, density and aperture, as well as determining the orientation of the horizontal stress field it is possible to interpret the fracture component of the well permeability. This has implications both for well targeting and reservoir modelling.

The recent use of high temperature acoustic formation imaging technology (AFIT) can provide the necessary fracture and stress data to assess the contribution of fractures to feed zone permeability. As part of an ongoing AFIT logging program at Wairakei, data has been collected from the open hole of a number of deep wells in the southern part of the field. The location of feed zones in these wells has been interpreted from the completion test data and then correlated with AFIT fracture density and aperture data to provide more accurate feed zone depths and to characterise the nature of the permeability. Only fractures with optimal orientation within the local stress field are considered as potentially open to fluid flow. While the correlation between feed zones and fracture density is poor, good correlation is observed with the location of individual wide-aperture fracture zones. These zones may represent significant flow paths in the reservoir.

1.0 INTRODUCTION

Recent deep drilling at Wairakei in the Karapiti South reinjection area has drilled beyond the relatively well-understood Waiora Formation and into the Tahorakuri formation, encountering previously unknown deep permeable zones around 2000-2500m depth. The nature of permeability in these zones and the controls on that permeability are of interest both for the reinjection strategy at Wairakei as well as understanding the nature of the connection between Wairakei and Tauhara geothermal systems.

The acoustic formation imaging tool (AFIT) or 'borehole televiewer' has provided a fracture dataset for the deep sections of these wells. Of the hundreds of fractures imaged only a small number will be permeable as fractures in the well bore wall need to also extend a significant distance beyond the well bore and be interconnected. Correlation with feed zones identified from completion testing enables the identification of fractures associated with permeability.

The spatial extent and orientation of these permeable fractures is providing new insights into the mechanics of the reservoir.

2.0 RESERVOIR SETTING

Pressure interference between the neighbouring Wairakei and Tauhara geothermal fields and the fluid geochemistry indicate that they are separate fields with separate upflows which are hydrologically connected at more than one level.

The deep wells WK317, WK404 and WK407 are located along the southern and eastern boundary of the Wairakei system, between the Wairakei and Tauhara systems (Figure 1). It is noteworthy that the overall permeability found in each of the wells

discussed is in the “high” to “very high” range, even for Wairakei, with values in the order of 100 t/h per bar and greater.

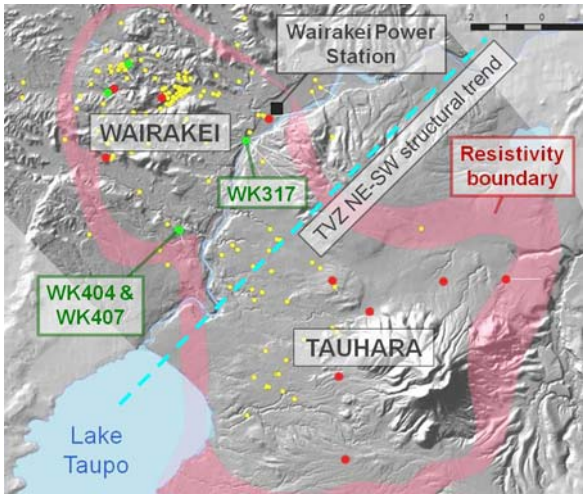

Figure 1: Well layout map for Wairakei-Tauhara. Wells in depth range 2500-3000m are in green, 1800-2500m in red, all others in yellow.

As illustrated in Figure 2 the active extensional tectonic setting of the Taupo Volcanic Zone (TVZ) has produced normal faulting oriented NE-SW throughout the region (Bignall et al, 2010), perpendicular to the orientation of the connection between Wairakei and Tauhara (Figure 1).

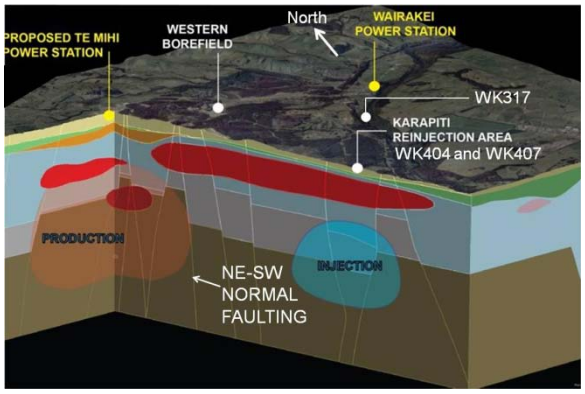

Figure 2: 3D geological model of the Wairakei system. Waiora Formation in pale blue and pink, Tahorakuri Formation in brown and rhyolite lavas in red.

Wairakei and Tauhara have distinct pressure-depth profiles at shallow depths (Figure 3). While no deep drilling has been completed at Tauhara, projection of the shallow pressure gradient predicts intersection with the Wairakei pressure gradient around minus 2500mRL, implying a permeable connection around this level.

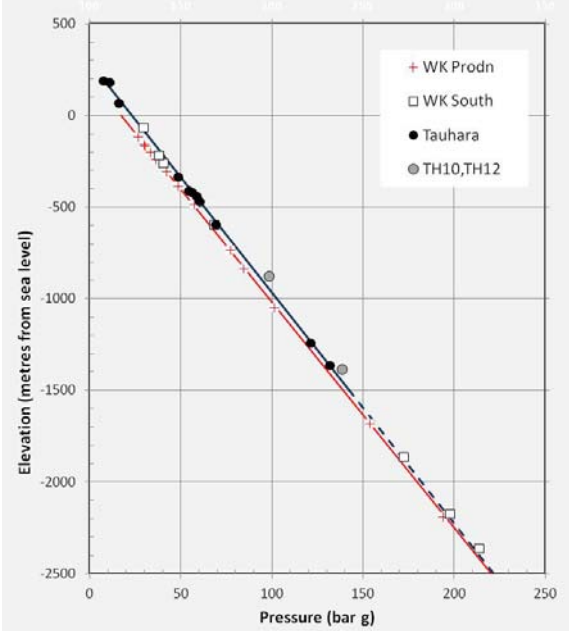

Figure 3: Pressure-depth profiles for Wairakei and Tauhara fields.

3.0 GEOLOGIC SETTING

The two major geologic formations relevant to this study are described below, from Bignall et al (2010) and the stratigraphic relationship between the formations is illustrated in Figure 4.

3.1 Waiora Formation

This is a thick volcanic sequence of non-welded/welded ignimbrite, tuff and breccia, with interlayered mudstones and siltstones, containing both rhyolite and andesite lavas.

The current understanding of permeability in the Waiora Formation is that is it is controlled by flow unit boundaries, particularly rhyolite lava boundaries.

3.2 Tahorakuri Formation

This is a pumiceous lithic tuff with intercalated partially welded ignimbrite. The tuff contains pumice, rhyolite lava and siltstone. Minor occurrences of the Waikora Formation greywacke-pebble conglomerate are intercalated with the Tahorakuri Formation.

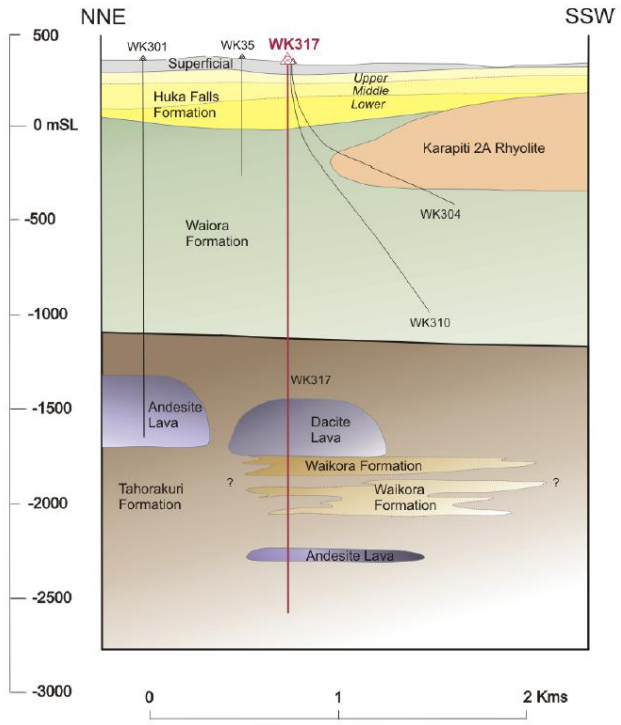

Figure 4: Cross-section in the vicinity of WK317 modified from Milicich et al (2010).

4.0 ACOUSTIC FORMATION IMAGING

4.1 Data acquisition

The AFIT tool is an acoustic borehole televiewer that is capable of operation in conditions ≤300°C. Developed by Advanced Logic Technology (ALT) in Europe it is operated in New Zealand by Tiger Energy Services (TES).

As the AFIT tool is lowered and raised in the well an acoustic transducer emits a sonic pulse. This pulse is reflected from a rotating, concave mirror in the tool head, focusing the pulse and sending it out into the borehole. The sonic pulse travels through the borehole fluid until it encounters the borehole wall. There the sonic pulse is attenuated and some of the energy of the pulse is reflected back toward the tool. This is reflected off the mirror back to the receiver and the travel time and amplitude of the returning sonic pulse is recorded. Through the use of the rotating mirror (≤5 rev/sec) 360° coverage of the inside of the borehole wall can be obtained.

4.2 Data set acquired

Planar geological features such as fractures can be observed as sinusoids on the final imaged data set (Figure 5). Accelerometers and magnetometers within the tool allow accurate structural measurements (strike and dip) to be obtained using processing software RECALL™. Further characterization of geological features (e.g. high or low amplitude, fracture density, fracture aperture) is also carried out using this software. The final dataset obtained is a spreadsheet including fracture depth, type, dip, dip direction and aperture.

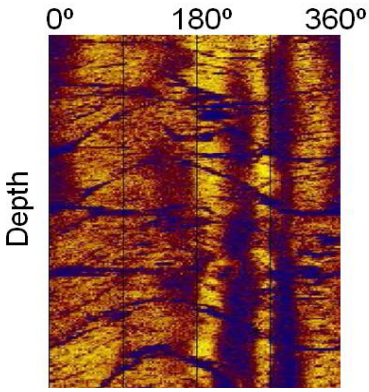

Figure 5: Example of AFIT amplitude response with sinusoidal intersection of fracture plane with wellbore.

4.3 Filters applied for this study

Before attempting to correlate fractures with the permeable zones from the completion test a number of filters are applied to the dataset in order to ensure that only fractures potentially open to fluid flow are included.

4.3.1 Confidence filter

Fractures in the dataset are classified as low confidence if their shape or existence is unsure. To lend a greater degree of confidence to the conclusions of this study, the low confidence fractures are filtered from the dataset.

4.3.2 Amplitude filter

Fractures with a low amplitude signal (dark) on an acoustic image are often interpreted as open. However these dark fractures may also be filled with sulfide minerals and so close attention is paid to alteration geology to distinguish these from other dark fractures. A fracture with a high amplitude signal (bright) is often interpreted as a closed fracture as the high amplitude signal can be attributed to a hydrothermal mineral fill. For the purposes of this study all high amplitude fractures are filtered from the dataset.

4.3.3 Azimuth filter

The maximum horizontal stress in the Taupo Volcanic Zone is generally oriented NE-SW as the orientation of the extension in this rift basin (and hence the minimum horizontal stress) is oriented NW-SE. The exact maximum horizontal stress orientation Sh_{max} at the well can be determined directly from measurement of drilling induced tensile fractures (DITF, Figure 6) observed on the AFIT

image. The orientation of Sh_{max} ranges between 035 and 045º in the Wairakei wells imaged to date (Table 1).

Table 1: Summary of Sh_{max} orientations

Well	Sh_{max} orientation
WK317	045º
WK404	045º
WK407	035º

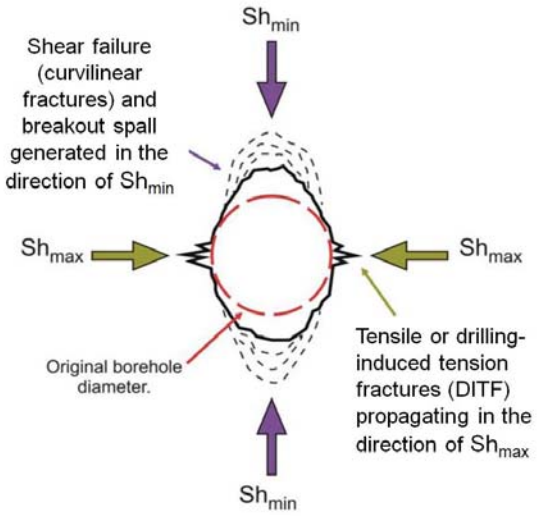

Figure 6: Schematic of relationship between tensile fracturing and maximum horizontal stress (modified from Dart and Zoback, 1989).

Only fractures with strike orientations that lie parallel to sub-parallel with the Sh_{max} orientation are likely to experience recurrent dilational fracture slip and hence ensure persistent permeability along the structure. The mechanisms for this are described in Davatzes and Hickman (2010). For each well two datasets are considered which contain fracture strike orientations within 45º and then 30º of Sh_{max}.

4.3.4 Filter summary

Table 2: Summary of fracture count at various stages of the filtering process

Dataset description	WK317 # fractures	WK404 # fractures	WK407 # fractures
All fractures (unfiltered)	846	963	912
After confidence +amplitude filters	663	840	634
After azimuth filter 45º from Sh_{max}	544	632	557
After azimuth filter 30º from Sh_{max}	440	511	455

4.4 Very wide aperture fracture zones

Some very wide, dark, low amplitude features are encountered with apertures of 0.5m or more. These are clearly not single fractures but more likely to be fracture zones. Hence in the raw dataset they are presented as one fracture with a certain width, and two orientations, one each for the upper and lower boundaries. For the purposes of graphing the data, these fracture zones are considered as one fracture, and the orientations of the boundaries are averaged to give a representative orientation across the implied fracture zone. This data processing step must be remembered as it is reversed later in the process as these wide-aperture zones usually correlate closely with permeability and require more detailed inspection.

5.0 CORRELATION OF AFIT DATA TO PERMEABLE ZONES

The completion test reveals locations of permeable zones in the well. Integration of the AFIT dataset with the completion test data, particularly the injection temperature and spinner profiles, resulted in the refinement of those feed zone locations. In some cases the feed zones were subdivided, widened or narrowed, or new ones added.

5.1 Fracture density

It was initially hypothesized that permeable zones would have a good correlation with areas of high fracture density. However it was revealed that fracture density is too dependent on the image quality, which is dependent on many factors including the acoustic properties of the fluid in the well bore and well bore shape (McNamara, 2010). Initial comparisons of WK404 fracture density with feed zone locations (Figure 7) reveal no correlation. A marked increase in fracture density in the lower half of the logged interval was attributed to improved image quality there (green and yellow) compared to poorer image quality in the upper half (orange and red) and hence a greater number of fractures being imaged and identified with confidence. All three sections of the image identified as being of high quality (green) coincide with significant peaks in the fracture density. It can therefore be concluded with confidence that the fracture density is significantly dependent on image quality. It is therefore not viable to correlate fracture density to the feed zones with high confidence.

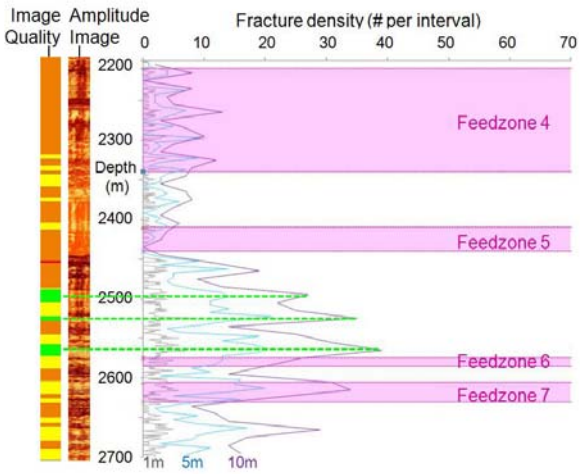

Figure 7: WK404 fracture density (1, 5 and 10m intervals) with feed zones interpreted from completion testing (pink) and image quality (green=good, yellow=moderate, orange=poor, red=bad).

5.2 Fracture aperture

The next attempt at correlation to the feed zones was made using the fracture aperture (Figure 8). It can be seen that the correlation is very good with most wide-aperture fractures coinciding with existing feed zones. This correlation is further improved by tightening the azimuth filter to within 30º of Sh_{max} from 45º which removes a number of fractures outside defined feed zones (grey) while all significant fractures within feed zones remain (red).

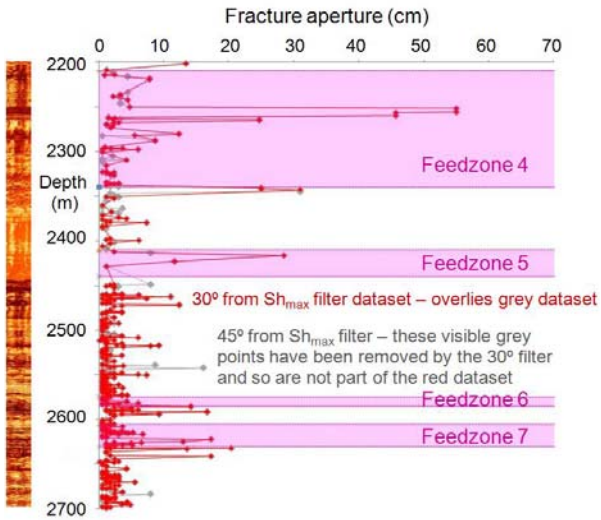

Figure 8: WK404 fracture aperture with feed zones interpreted from completion testing (pink). Grey data points (45º azimuth filter) are overlain by red data points (30º azimuth filter).

A few wide-aperture fractures fall just outside feed zones. It is very likely that this small depth discrepancy is due to factors such as wireline stretch which contribute to an uncertainty of up to a few metres in different downhole logging runs. Also as the spinner fluid velocities are measured after the installation of the slotted liner there is some smearing-out of the spinner profile as it takes some distance for the flow to fully develop after passing a feedzone. A process of adjustments to the defined extent of the feed zones attempts to take account of these factors. In the three wells discussed, this process included the subdivision of feed zones, addition of new feed zones and slight adjustment of feed zone boundaries.

5.2.1 WK404

In WK404 feed zone 4 was subdivided into four (FZ 4a-d) based on the very close correlation between injection temperature profile increases and wide aperture fractures (Figure 9). These temperature profiles are the most useful for identifying the upper feed zones (above 2400m) as at these depths the pressure in the wellbore is less than the reservoir pressure, causing hot fluids to flow from the reservoir into the well at permeable depths.

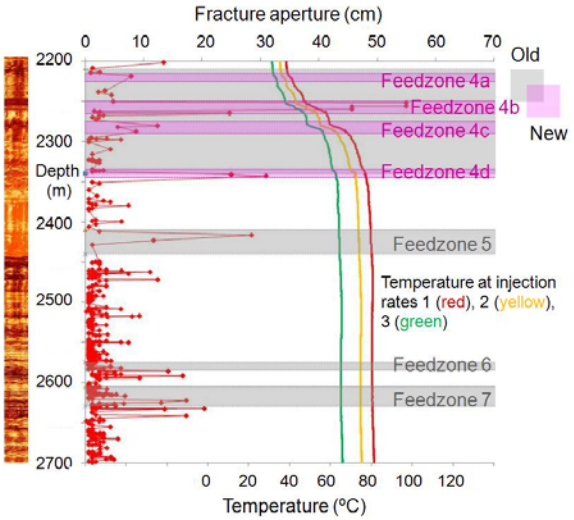

Figure 9: WK404 upper feed zone refinement using fracture aperture and temperature profiles. Old feed zones (grey) are overlain with new feed zones (pink).

The lower feed zones are based on the fluid velocity derived from multiple spinner profiles which is useful for identifying deeper feed zones as the higher pressure in the well bore compared to the reservoir results in the flow of water out of the well at permeable depths, resulting in distinct down-steps in the fluid velocity. FZ6 and 7 have been down-shifted slightly to incorporate wide aperture fractures while

still being consistent with the spinner profile (Figure 10).

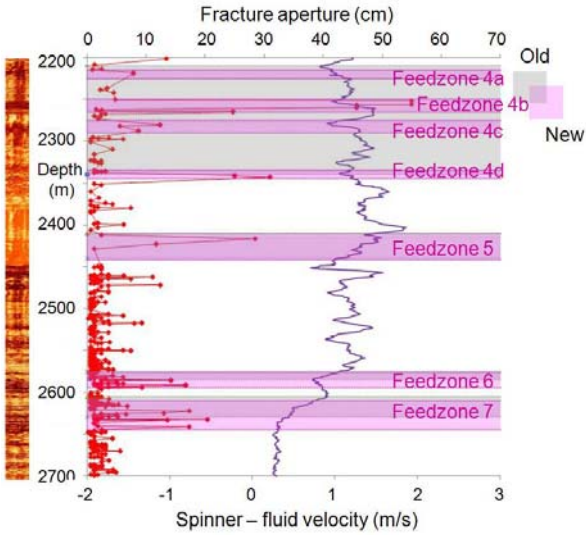

Figure 10: WK404 lower feed zone refinement using fracture aperture and spinner fluid velocity profile. Old feed zones (grey) are overlain with new feed zones (pink).

This process of refinement is summarized in Table 3 and identified a total of 7 discrete feed zones in the depth interval of interest.

Table 3: Summary for WK404 of feed zones and redefined feed zones

Feed Zone Name	Depth range (m)	New Feed Zone name	New depth range (m)	Comments
4	2210-2340	4a	2215-2225	Subdivided from FZ4 based on injection temperature profiles and fracture aperture
		4b	2251-2266	
		4c	2275-2290	
		4d	2335-2345	
5	2410-2440	5	2411-2442	Little change
6	2575-2585	6	2577-2595	Down-shifted slightly based on spinner profile and fracture aperture
7	2605-2630	7	2610-2645	Down-shifted slightly based on spinner profile and fracture aperture

5.2.2 WK317

In WK317 AFIT fracture data was obtained over the interval 2200-2700m. It can be seen (Figure 11) that there is a good correlation between the fracture aperture and the feed zones defined from the completion test. The process of refinement is summarized in Table 4 and includes the addition of a feed zone not previously identified in the completion test. This was based on the existence of a very wide aperture fracture which was not correlated with any of the existing feed zones. Closer inspection revealed an anomaly at this depth in the temperature profiles during heat-up (blue) and so a feed zone was added. This location is too deep to be detected by the injection temperature profiles and not deep enough to be detected by the spinner profile.

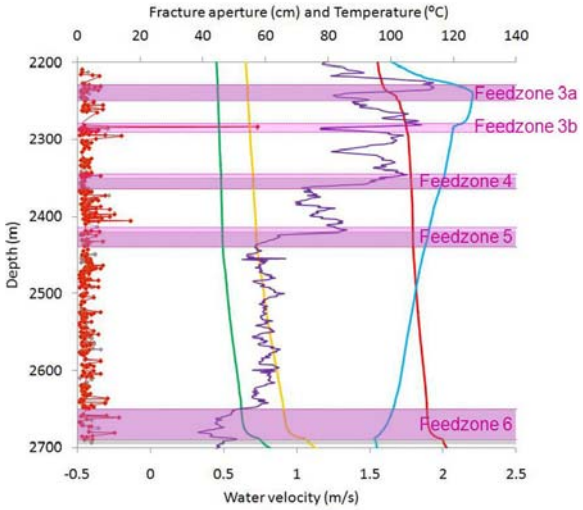

Figure 11: WK317 feed zone refinement using fracture aperture, spinner fluid velocity profile and temperature profiles. Old feed zones (grey) are overlain with new feed zones (pink).

Table 4: Summary for WK317 of feed zones and redefined feed zones

Feed Zone Name	Depth range (m)	New Feed Zone name	New depth range (m)	Comments
3	2230-2250	3a	2230-2250	No change from original FZ3
		3b	2280-2290	Added based on coincidence of wide aperture fracture with temp anomaly in heat up runs
4	2350-2365	4	2345-2365	Widened slightly
5	2420-2440	5	2415-2440	Widened slightly
6	2650-2695	6	2650-2690	Narrowed slightly

5.2.3 WK407

In WK407 AFIT fracture data was obtained over the interval 2200-2920m. It can be seen that there is a good correlation between feed zones from the completion test and the wide aperture fractures (Figure 12). Nine individual feed zones were identified in this well with only minor changes made during the refinement process, summarized in Table 5.

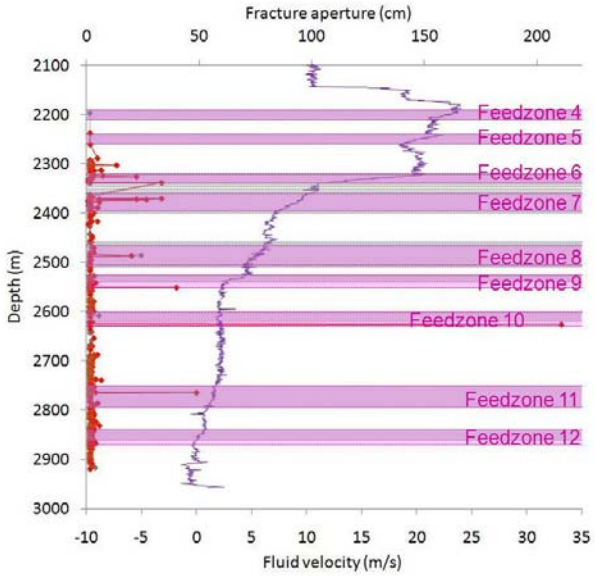

Figure 12: WK407 feed zone refinement using fracture aperture and spinner fluid velocity profile. Old feed zones (grey) are overlain with new feed zones (pink).

Table 5: Summary for WK407 of feed zones and redefined feed zones

Feed Zone Name	Depth range (m)	New Feed Zone name	New depth range (m)	Comments
4	2190-2210	4	2190-2210	No change, insufficient fracture data
5	2240-2260	5	2240-2260	No change, insufficient fracture data
6	2320-2345	6	2321-2340	Narrowed slightly based on spinner and aperture
7	2350-2400	7	2360-2395	Narrowed slightly based on spinner and aperture
8	2460-2510	8	2465-2505	Narrowed slightly based on spinner and aperture
9	2525-2540	9	2525-2552	Widened and deepened slightly based on spinner and apertures
10	2600-2620	10	2601-2630	Widened and deepened slightly based on spinner and apertures
11	2750-2795	11	2750-2795	No change
12	2840-2860	12	2840-2870	Widened and deepened slightly based on spinner and apertures

5.3 Orientation of fractures within refined feed zones

Comparison of the orientation of the whole fracture dataset to the fractures within feed zones and then the individual wide aperture fractures is required to identify any systematic differences between these datasets.

5.3.1 WK404

A rose diagram of the fracture orientations in redefined feed zone 7 of WK404 (Figure 13) is a good representative diagram for many of the feed zones in this study as it exhibits features common to many feed zones. The dominant NE-SW orientation of the fractures is clearly shown, as is a minor group of fractures oriented NW-SE at right-angles to the dominant orientation. The majority of fracture planes dip to the northwest.

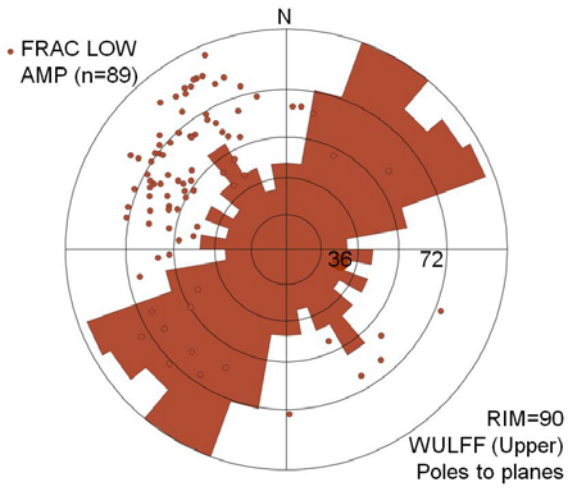

Figure 13: Rose diagram of fracture orientations in redefined feed zone 7 of WK404.

For the purposes of summarizing the data, all strike angles reported in Tables 6-11 have been projected

into the first and second quadrants (0-90º and 90-180 º) before averages were calculated.

Table 6: Summary for WK404 of orientations of all fractures within redefined feed zones

FZ	From (m)	To (m)	# Frac	Av Dip	SD Dip	Av Strk	SD Strk
4a	2215	2225	2	72.4	0.1	46.7	1.2
4b	2251	2266	10	78.0	6.9	65.0	10.4
4c	2275	2290	5	72.0	4.1	49.3	21.1
4d	2335	2345	8	80.4	4.9	47.4	18.1
5	2411	2442	5	73.4	10.0	43.6	17.0
6	2577	2595	42	66.7	11.2	49.8	13.5
7	2610	2645	59	69.0	10.3	43.2	16.9
All	2200	2700	963	66.0	12.6	69.2	46.3
30° filt	2200	2700	511	67.2	12.0	45.1	16.0

The average dip for all fractures in the WK404 dataset is moderate to steep at 66.0º. This average dip is slightly increased to 67.2º by the process of filtering out all fractures not optimally oriented to Sh_{max}. In almost all cases the average dips within the feed zones are slightly increased again from the filtered dataset value of 67.2º.

The average strike for all fractures in the dataset is 69.2º and decreases to 45.1º with the application of the azimuth filter. This is not surprising as this filter will bias the dataset towards orientations close to Sh_{max} which for WK404 is 45º. The average strike in all the feed zones are then very close to this overall value, within 5º, with the exception of FZ4b which is within 20º.

Consideration must be given to the individual wide-aperture fractures considered to be responsible for the permeability based on the correlations observed. The orientations of these specific fractures (Table 7) may present a different picture to the averages across the feed zones.

Table 7: Summary for WK404 of orientations of wide-aperture fractures within redefined feed zones

Feed Zone Name	# fracture zones	Average dip of boundaries	Average strike of boundaries
4a	2	72.4	46.7
4b	3	80.0	68.5
4c	2	73.7	57.8
4d	2	82.7	54.1
5	2	77.3	35.1
6	5	66.7	37.2
7	8	71.4	45.1

It can be seen from Table 6 and Table 7 that the average dip of the specific wide-aperture fractures in the feed zones is slightly higher than for the average of all fractures in those feed zones. The range of dip of wide aperture fractures is 66.7º to sub-vertical at 82.7 º.

No clear trend can be observed in the strike other than to note that they are within 10° of Sh_{max} with one exception.

5.3.2 WK317

The same trend as WK404 is observed here as average dips increase from the overall WK317 dataset to the 30º filtered dataset and then the feed zone datasets and then wide aperture fractures (Tables 8 and 9).

Table 8: Summary for WK317 of orientations of all fractures within redefined feed zones

FZ	From (m)	To (m)	# Frac	Av Dip	SD Dip	Av Strk	SD Strk
3a	2230	2250	24	73.4	7.4	39.9	15.5
3b	2280	2290	15	79.1	6.1	41.8	8.7
4	2345	2365	21	75.0	8.9	30.0	10.9
5	2415	2440	19	76.8	9.9	40.2	12.3
6	2650	2690	17	74.2	8.2	42.4	19.8
All	2200	2700	846	72.7	9.5	59.3	47.3
30° filt	2200	2700	440	73.9	8.7	41.6	16.1

The strike trend of WK404 is also observed here, the average strike for all fractures in the dataset is 59.3º and decreases to 41.6º with the application of the azimuth filter. The average strike in all the feed zones are then very close to this overall 41.6º value with the exception of FZ4 which has an average strike of 30.0º.

Table 9: Summary for WK317 of orientations of wide-aperture fractures within redefined feed zones

Feed Zone Name	# fracture zones	Average dip of boundaries	Average strike of boundaries
3a	5	73.2	52.1
3b	4	80.6	36.3
4	1	70.1	48.8
5	3	74.8	44.2
6	4	77.3	43.3

5.3.3 WK407

WK407 data (Tables 10 and 11) generally demonstrates the same trends observed in WK404 and WK317 of progressively increasing average dip and average strikes close to Sh_{max}.

Table 10: Summary for WK407 of orientations of all fractures within redefined feed zones

FZ	From	To	#	Av	SD	Av	SD

	(m)	(m)	Frac	Dip	Dip	Strk	Strk
4	2190	2210	0				
5	2240	2260	0				
6	2321	2340	19	77.4	9.3	37.2	7.6
7	2360	2395	25	78.8	7.7	45.2	14.8
8	2465	2505	8	74.0	10.4	28.0	9.5
9	2525	2540	11	65.9	16.0	26.1	17.7
10	2601	2630	18	72.8	7.7	41.1	10.8
11	2750	2795	39	71.9	10.4	34.9	13.1
12	2840	2870	34	71.2	11.0	26.0	12.3
All	2200	2920	912	73.4	11.0	57.1	45.0
30° filt	2200	2920	455	74.2	10.3	34.0	14.4

Table 11: Summary for WK407 of orientations of wide-aperture fractures within redefined feed zones

Feed Zone Name	# fracture zones	Average dip of boundaries	Average strike of boundaries
4	0		
5	0		
6	3	83.7	39.1
7	5	82.4	47.7
8	2	63.6	8.8
9	1	74.2	60.3
10	1	71.5	27.6
11	1	65.6	23.9
12	0		

5.3.4 Discussion of increasing dip

It is observed in the majority of cases that the average dip increases progressively as the dataset is narrowed from the full dataset to the 30º azimuth filtered dataset to only those fractures within the redefined feed zones, and then to only those wide-aperture fractures within those zones. While this trend represents small changes in average dip which are within the statistical variability of the system, it does hold true for the majority of cases.

In these areas of the Wairakei system the overall fracture orientation is steeply dipping and dominated by an orientation parallel to the maximum horizontal stress. On the basis of the above observations of average dip it can be stated that the steeper fractures are more likely to be correlated with permeability in the well.

5.3.5 Discussion of average strikes

With few exceptions, permeable feed zones in this study are associated with wide-aperture fracture zones oriented approximately NE-SW along the regional structural trend. This is apparently at odds with the orientation of the known larger-scale deep permeable connections between Wairakei and Tauhara, which are aligned NW-SE. This requires further work and the minor group of fractures oriented NW-SE (Figure 13) is of interest and may be significant. These fractures may be related to an old tectonic regime or represent transform fractures between fractures in the dominant set.

5.4 Geological considerations

Although the heterogeneity within the Tahorakuri Formation has not been fully explored, at this stage in WK317 there appears to be little stratigraphic control on permeability. Permeability is found within both the Tahorakuri Formation and the Waikora Formation and not necessarily at boundaries. While a minor feed exists near the upper boundary of the dacite lava, no permeability is associated with the deeper andesite lava. Heterogeneity within the Tahorakuri Formation may explain the locations of some feed zones and this will be the subject of further study. However at this stage the data suggests that stratigraphy (and thus any primary permeability) is not a significant control on the deep permeability and it is instead dominated by secondary fracture permeability. Quartz and calcite are present in the hydrothermal alteration mineral assemblage in all these deep formations, consistent with the findings of Davatzes and Hickman (2010) that alteration minerals such as these will aid the maintenance of permeability through dilational fracture slip processes.

The Waikora Formation is not present in WK404 and WK407. No significant lithological changes are noted in the interval of interest in these wells, all feed zones are located within Tahorakuri Formation.

6.0 CONCLUSIONS

Fracture data from the AFIT tool can be used in combination with completion test data to refine the locations of feed zones in geothermal wells.

The orientation of fractures within redefined feed zones allows an assessment of their contribution to permeability.

At Wairakei the permeable zones within the Tahorakuri and Waikora Formations identified in wells WK317, WK404 and WK407 are dominated by secondary fracture permeability controlled by the extensional tectonic stress field.

Findings from the studied wells in this part of the Wairakei geothermal system show that fractures open to fluid flow are oriented perpendicular to the connection with Tauhara geothermal system.

Future work planned for AFIT data:

- Closer study of the NW-SE oriented fracture set which is aligned with the Wairakei-Tauhara connection.
- Investigation of possible correlations between the heterogeneity of the Tahorakuri Formation and the location of feed zones to determine any lithological control on permeability.
- Correlation of AFIT image to known fractures from a fully cored well will improve identification of fractures from images for future wells where core is not available.
- Comparison of AFIT fracture trends to any existing or future microseismic studies to investigate any correlation between the two.

7.0 REFERENCES

Bignall, G., Milicich, S., Ramirez, E., Rosenberg, M., Kilgour, G. and Rae, A. (2010), "Geology of the Wairakei-Tauhara Geothermal System, New Zealand", *Proceedings World Geothermal Congress 2010*, Bali, Indonesia, 8p.

Dart, R. and Zoback, M. (1989), "Wellbore breakout stress analysis within the central and eastern continental United States", *Log Analyst*, **30**, 12-25.

Davatzes, N.C. and Hickman, S.H. (2010), "The Feedback Between Stress, Faulting, and Fluid Flow: Lessons from the Coso Geothermal Field, CA, USA", *Proceedings World Geothermal Congress 2010*, Bali, Indonesia, 15p.

McNamara, D. (2010), "AFIT Image Interpretation: Well WK317, Wairakei Geothermal Field (2200-2700m)", *Confidential GNS Science Letter Report 2010/140LR.* `

McNamara, D. (2010), "Structural Interpretation of Acoustic Borehole Images from Well WK404, Wairakei Geothermal Field", *Confidential GNS Science Consultancy Report 2010/160*.

McNamara, D. and Massiot, C. (2010), "Structural Interpretation of Acoustic Borehole Images from Well WK407, Wairakei Geothermal Field", *Confidential GNS Science Consultancy Report 2010/287*.

Milicich, S., McNamara, D., Rae, A. and Rosenberg, M. (2010), "Geology of Injection/Exploration Well WK317, Wairakei Geothermal Field", *Confidential GNS Science Consultancy Report 2010/28*.

Rae, A., Hitchcock, D. and Bignall, G. (2011), "Combined Geological Report for Injection Wells WK403, WK404 and WK407, Karapiti South, Wairakei Geothermal Field", *Confidential GNS Science Consultancy Report 2011/01*.